CHAPTER 3
METHODOLOGY

3.1 Materials

3.1.1 Ordinary Portland Cement

This study used ordinary Portland cement Type I (OPC) from the Siam Cement Company. The physical properties and chemical composition are shown in Table 3.1 and 3.2, respectively. The chemical composition was investigated by X-ray fluorescence (XRF; WDXRF PW2400).

Table 3.1 Physical properties of raw materials.

Sample	Specific Gravity	Retained on Sieve No. 325 (% retained)	Median Particle Size, d_{50} (μm)
OPC	3.13	14	-
Rice husk ash (RHA)	2.13	31	28
River sand	2.59	-	94.7
Al-containing waste (AW)	3.05	33	-
Quick lime (CaO)	2.34	-	-

3.1.2 River Sand

River sand in this study was used as a fine aggregate and was ground to the average particle size of nearly 100 μm in a ball mill. The physical properties of river sand are also given in Table 3.1. The specific gravity of the river sand was measured by following ASTM C128 [47].

3.1.3 Lime

This study used quick lime (CaO), which was obtained from Kowit Lime Saraburi Industry. The physical properties of quick lime are given in Table 3.1, and the chemical composition is shown in Table 3.2.

Table 3.2 Chemical composition of raw materials.

Chemical properties	OPC	RHA	Quick lime	AW
CaO	66.20	0.70	94.7	10.1
SiO_2	18.80	92.80	0.89	3.37
Al_2O_3	4.65	0.15	0.11	81.1
Na_2O	0.20	0.08	-	3.28
Fe_2O_3	3.22	0.17	0.10	1.09
MgO	0.79	0.77	2.61	6.57
P_2O_5	0.07	1.07	0.02	0.07
K_2O	0.75	3.35	0.01	0.10

3.1.2 River Sand

River sand in this study was used as a fine aggregate and was ground to the average particle size of nearly 100 μm in a ball mill. The physical properties of river sand are also given in Table 3.1. The specific gravity of the river sand was measured by following ASTM C128 [47].

3.1.3 Lime

This study used quick lime (CaO), which was obtained from Kowit Lime Saraburi Industry. The physical properties of quick lime are given in Table 3.1, and the chemical composition is shown in Table 3.2.

3.1.4 Aluminium Powder

Aluminium powder was supported from the Super Block Company Limited. The physical properties of aluminium powder are given in Table 3.3.

Table 3.3 Physical properties of aluminium powder.

Material	Purity (%)	Median Particle Size, d_{50} (μm)
Aluminium powder	94	34

3.1.4 Al-containing Waste (AW)

Al-containing waste was obtained from SRI Metal Products. The physical properties and chemical composition of AW are given in Tables 3.1 and 3.2, respectively. Al-containing waste is classified into three finenesses which are low, medium and high, and are those having particles retained on sieve no. 325 greater than 45 (AC), between 45-34 (AM) and lower than 34% (AF), respectively. The metallic aluminium content of AW was determined by measuring the volume of hydrogen gas produced during the reaction between metallic aluminium and hydrated lime, as shown in equation 3.1.

$$2Al + 3Ca(OH)_2 + 6H_2O \rightarrow 3CaOAl_2O_3{\cdot}6H_2O + 3H_2 \quad (3.1)$$

According to Eq. 3.1, 1 mol of Al produces 1.5 mol of H_2 and 1 mole of ideal gas is equal to 22.41 liters where the molar mass of Al equals 26.98 grams. This relationship between the volume of hydrogen gas (V_{H2}) produced and the amount of metallic aluminium (m_s) in the residue is identified in Eq. 3.2.

$$V_{H_2} = \left[\frac{m_s}{26.98\frac{g}{mol}}(1.5)\left(22.41\frac{l}{mol}\right)\right] \quad (3.2)$$

The measurement of the metallic aluminium content in AW was determined by using the calibration curve of pure metallic aluminium. The content of gas released was measured at 1, 2, 3, 4, 5, 10, 20, 30, 40, 50, 60 min and then every 30 min until 150 min.

3.1.5 Rice Husk Ash

RHA in this study was synthesized in a laboratory, and the rice husk was obtained from Chai Wanich Rice Mill. The RHA synthesis was made by filling a flat steel plate with rice husk and this was then put into an electric furnace. RHA was burnt from room temperature to 650°C for 1 hour, after which the temperature was stable for 1 hour and then allowed to cool. After burning, RHA was taken out of the electric furnace at a temperature of 500°C for immediate cooling. The RHA was then ground in a ball mill with 63 steel balls (4.6 kg) for 3 h to retain on sieve No.325 under 34% by weight as followed by ASTM C618 [48]. The physical properties of RHA are given in table 3.1 and the chemical properties of RHA were observed by using XRF, which is given in table 3.2. In

addition, the crystallinity of RHA was characterized by using an X-ray diffractometer (XRD).

3.2 Experimental Procedures

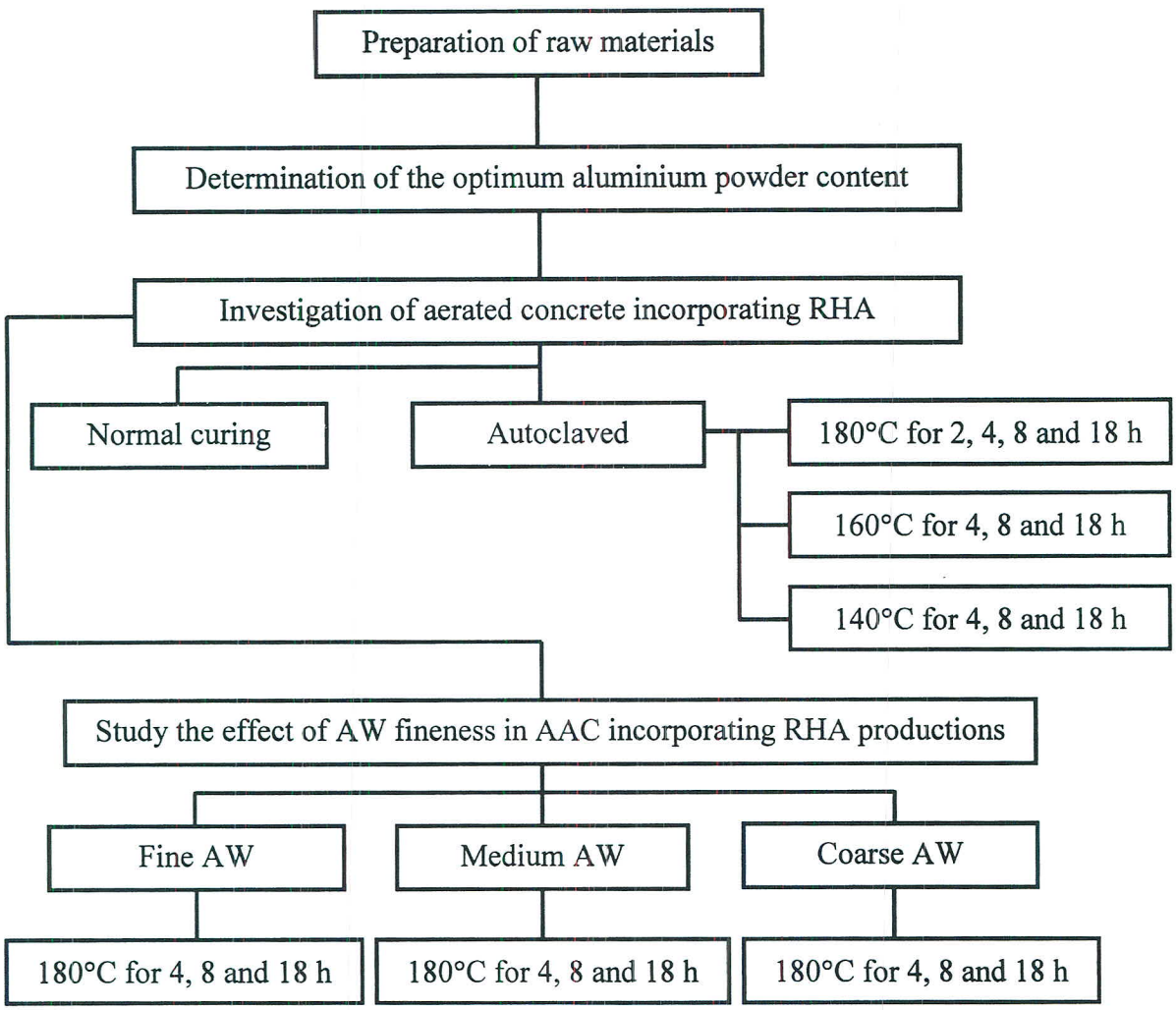

Figure 3.1 Experimental scheme.

3.3 Sample Preparation

Tables 3.4-3.6 represent the mix proportions used for Chapter 4-6, respectively. The Water/Binder (W/B) ratio for each mix proportion was determined using the flow table method in accordance with ASTM C109 [49]. Firstly, the ingredients for each proportion of mix were calculated for a set of six samples and then weighed. The solid

ingredients, i.e. OPC, CaO, sand, RHA and aluminium powder, were poured into a Horbart Mixer and mixed at the first speed for 1 min. Water was then added and the ingredients were mixed again at the first speed for 1 min followed by the second speed for 30 sec. After that, the slurry was poured into 5 cm cube steel moulds following ASTM C109 [49] and left until the pore-forming reaction was completed. The reaction time for each mix proportion is summarized in Tables 3.7 and 3.8. The expanded parts of the samples are cut with a nylon fishing line.

Under non-autoclave aerated concrete, the samples were cured in a steel mould for 1 day and then removed and placed into water for 7, 14 and 28 days. The samples that were autoclave cured were preheated in an oven at 40°C for 3 hr to achieve the desired setting and volume stability. After the preheating process, and while the samples were still soft they were removed from the steel mould and placed into an autoclave at various temperatures and times, as summarized in Fig. 3.1. Under autoclaved curing conditions, the temperature was increased at the rate of 15°C per 10 min until the desired temperature was reached and maintained with a variation of ±5°C over the desired length of time. After that, the temperature was dropped at the same rate until it reached 50°C and the samples were then removed from autoclave.

After curing, some samples were dried in an oven at 40°C for 24 hr to remove the excess water for testing compressive strength. The other samples were subjected to drying in an oven at 105°C for 24 hr to determine the dry density.

Table 3.4 Mix proportions of aerated concrete.

Samples	OPC (wt%)	CaO (wt%)	Sand (wt%)	Aluminium powder (wt% of Binder)	W/B ratio
0	45	5	50	0	0.65
0.3	45	5	50	0.3	0.65
0.5	45	5	50	0.5	0.65
0.7	45	5	50	0.7	0.65
0.9	45	5	50	0.9	0.65

Remark: S and W are the weights of sand and water, respectively, and B is the weight binder (OPC+Lime).

Table 3.5 Mix proportions of aerated concrete incorporating RHA.

Samples	OPC (wt%)	CaO (wt%)	RHA (wt%)	Sand (wt%)	Aluminium powder (wt% of Binder)	W/B ratio
CT	45	5	0	50	0.5	0.65
RHC25	45	5	12.5	37.5	0.5	0.78
RHC50	45	5	25	25	0.5	1.00
RHC75	45	5	37.5	12.5	0.5	1.22
RHC100	45	5	50	0	0.5	1.43

Table 3.6 Mix proportions of aerated concrete incorporating RHA and AW.

Samples	OPC (g)	CaO (g)	RHA (g)	Sand (g)	Aluminium powder (g)	AW (g)
CT	360	40	300	100	2.0	0
AWC5	360	40	300	100	1.9	10
AWC10	360	40	300	100	1.8	20
AWC15	360	40	300	100	1.7	30
AWC20	360	40	300	100	1.6	40

Table 3.7 The pore-forming reaction time for aerated concrete incorporating RHA.

Samples	Pore-forming time (min)
Control	35
RHC25	40
RHC50	45
RHC75	50
RHC100	55

Table 3.8 The pore-forming reaction time for aerated concrete incorporating RHA and AW.

AW replacement ratio (%)	Pore-forming time (min)		
	AWS	AWM	AWL
5	25	45	50
10	20	40	50
15	15	35	45
20	10	30	40

3.4 Microstructural Analysis

The mineralogical composition and microstructure of the samples cured under both conditions (moist cured and autoclaved) were investigated using an X-ray Diffractometer (XRD), a Scanning Electron Microscope (SEM) and an energy dispersive X-ray spectrometer (EDX). The XRD is used to observe the crystalline composition of the samples, which we investigate by using powdered samples. The SEM is used to image the sample's surface characteristics, which we investigate using a piece of a sample. The EDX is used to identify the amount and types of elements in the samples, which it is used with the SEM.

3.4.1 Scanning Electron Microscope (SEM)

A scanning electron microscope (SEM) is a type of electron microscope that is used to image a sample with a high energy beam of electrons in a raster pattern. The SEM has a large depth of field, a wide range of magnification (10 times to 1000000 times) and high spatial resolution (5 nanometers). It can also be used in conjunction with other techniques, such as the Energy Dispersive Spectrometry (EDS) and the Wavelength Dispersive Spectrometry (WDS) to identify the composition in a sample.

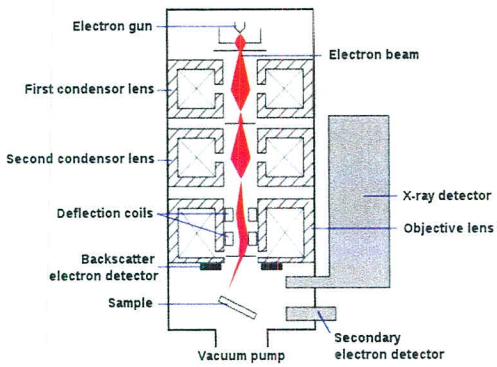

Figure 3.2 Schematic diagram of SEM [50].

In a typical SEM, an electron beam is emitted from an electron gun, and the electrons move into a vacuum column by accelerating the voltage in the range of 0-30 kV. The beam is focused by one or two condenser lenses to a spot about 0.4 nm to 5 nm in diameter and is passed through deflection coils, which in the final lens defects the beam in the x and y axes so that it scans in a raster fashion over a rectangular area of the sample surface. Finally, these signals are detected and evaluated by a computer. In my research, the SEM is used to image the sample surface and an Energy Dispersive X-ray Spectrometer (EDX) is used to identify the amount and types of elements.

3.4.2 X-ray Diffractometer (XRD)

An X-ray diffractometer (XRD) is a rapid analytical technique primarily used for the phase identification of a crystalline material and can provide details on unit cell dimensions. The fundamental principle of XRD uses Bragg's Law to observe the samples, as shown in Equation 3.3. When X-rays are incident on an atom with a stable wavelength, the diffraction angle is dependent on the lattice spacing in a crystalline sample. After that, these diffracted X-rays are found, processed and counted. In this research, we use an XRD to investigate the crystalline composition in powdered samples.

$$2d \sin\theta = n\lambda \tag{3.3}$$

Where d is the distance between atomic layers in a crystal.

λ is the wavelength of the incident X-beam.

n is an integer.

3.5 Physical and Mechanical Analyses

3.5.1 Compressive Strength

In concrete, compressive strength is the important factor. This is because the compressive strength of concrete is the main factor in designing the proportions of mix in the concrete. Although, AAC does not require high compressive strength, compressive strength is still the main factor. In this thesis, all samples used were 5×5×5 cm^3 for the compressive strength test and a set of five samples were used for each mix proportion and curing duration to determine compressive strength values following ASTM C109 [49]. The average value was reported to the nearest 10 psi (0.1 MPa) and the variation no more than 10%.

3.5.2 Dry density

Dry density was also tested in all samples under both curing conditions (cured in water and autoclaved) and a set of five samples was used for each mix proportion and curing duration. Dry density is calculated as follows:

Dry density = (Dry weight of sample)/(Dry volume of sample)

Dry samples were baked at a temperature of 105±5°C for 24 hours and then placed in desiccators to cool.

3.5.3 Thermal Conductivity

Thermal conductivity is used to measure the thermal transport properties of a material or component. In this study, thermal conductivity was determined on 30×30×5 cm^3 specimens in accordance with ASTM C518 [51] Heat Flow Meter Method using the Thermal Conductivity of Building and Insulating Materials Unit B480. This test method measures the thermal transmission through flat slab specimens between two parallel plates at constant but different temperatures, as shown in Fig. 3.3. The heat flux transducers at the end of each plate acted the converting device from heat transmission to electric potential and then the data was sent and collected by computer. The software, which was derived from Fourier's Law of heat conductivity as accordance in Equation 3.4, was used to calculate thermal conductivity, and thermal resistivity or thermal resistance and thermal conductance.

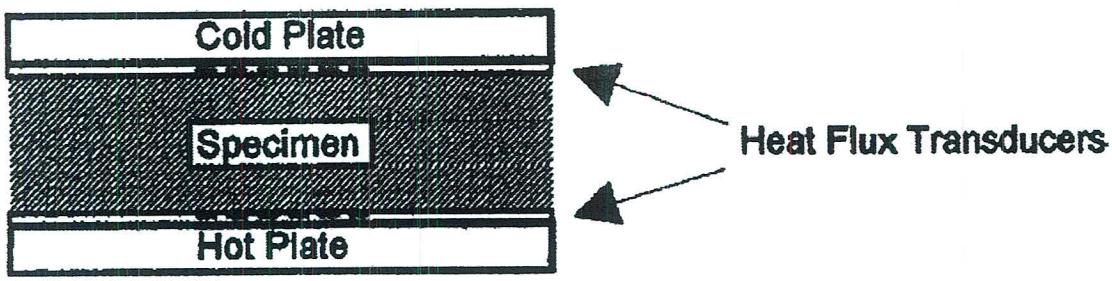

Figure 3.3 Heat flow meter apparatus [51].

$$\lambda = \frac{l_s \times [(k_1 + (k_2 \times \overline{T})) + ((k_3 \times (k_4 \times \overline{T})) \times HFM + ((k_5 + (k_6 \times \overline{T})) \times HFM^2)]}{dT} \quad (3.4)$$

Where λ is Thermal conductivity (W/mK)

l_s is Thickness of specimens (meters)

dT is Temperature difference across the specimen, T_1-T_2 (°C)

$\overline{T}$ is mean temperature, $\frac{(T_1+T_2)}{2}$ (°C)

HFM is Heat flow meter reading (mV)

k_1 is -21.2814

k_2 is 0.4101

k_3 is 4.9286

k_4 is 0.0048

k_5 is 0.0301

k_6 is 0.0002